Elsevier Editorial System(tm) for Fire Safety Journal
Manuscript Draft

Manuscript Number:

Title: On the Fluid Dynamics of the Make-Up Inlet Air and the Prediction of Anomalous Fire Dynamics in a Large-Scale Facility

Article Type: Research Paper

Keywords: make-up air, mechanical exhaust, CFD simulations, atrium, full-scale fire tests.

Corresponding Author: Dr Candido Gutiérrez-Montes,

Corresponding Author's Institution: University of Jaén

First Author: Candido Gutiérrez-Montes

Order of Authors: Candido Gutiérrez-Montes; Enrique Sanmiguel-Rojas, Dr; Manuel A. Burgos, Dr; Antonio Viedma, Professor

Abstract: The present paper is focused on the fluid dynamics of the make-up air at the vents in case of an atrium fire, its influence on the fire-induced conditions and the necessity of properly model it to obtain an accurate numerical prediction. For this aim, experimental data from two full-scale atrium fire tests conducted in a 20 m cubic facility, with venting conditions involving mechanical smoke exhaust and make-up air velocities larger than 1 m/s, and with different fire powers, are presented. Subsequent numerical simulations of these tests have been performed with the code Fire Dynamics Simulator v5.5.3. Two different approaches have been followed to simulate the make-up air inlet fluid dynamics, involving one domain which only considers the inside of the building and another which includes part of the outside. In the former simulations, anomalous phenomena around the fire appear, while the inclusion of the exterior domain provides with a completely different fluid dynamics inside the facility which agrees better with the experimental data. A detailed analysis of the fluid mechanics at the air inlet vents is conducted to explain these discrepancies. Finally, further simulations are performed varying the make-up area to assess the appearance of the aforementioned phenomenon.

University of Jaén

Department of Mechanical and Mining Engineering

Fluid Mechanics Division

12th May, 2011

Dear Professor José Torero:

Please find enclosed the full-paper "**On the Fluid Dynamics of the Make-Up Inlet Air and the Prediction of Anomalous Fire Dynamics in a Large-Scale Facility**" for possible publication in the International Journal Fire Safety Journal. The authors have read numerous papers from your journal related to the subject tackled at the present work, which have been source of knowledge, as well as published some research papers in it, and so we think the subject of the present work could fit some of the scopes of this journal and could be of your interest. The authors guarantee the originality of the work and think that contributes to the state-of-the-art of the study of fires within big volume buildings or atria. Specifically, this work is focused on the make-up air influence which is one of the most important issues to take into account when designing smoke exhaust systems. One of the most relevant contributions of this research is the presentation of new experimental data of fires within a new full-scale fire test facility for fire models validations. Additionally, a comparison of these experimental data with predicted results from numerical simulations carried out using one of the most extensively used fire field model, FDS, is presented.

Also attached you will find the figures as original graphics files.

We would greatly appreciate it if you begin the revision process of the above mentioned paper.

Kind regards,

Dr. Gutiérrez-Montes.

Dr. Cándido Gutiérrez Montes
Corresponding author

Email: cgmontes@ujaen.es
Fluid Mechanics Division
Department of Mechanical Engineering
University of Jaén
Campus Las Lagunillas
23.071 Jaén, Jaén (Spain)
Tel. +34-953-21.29.03
Fax +34-953-21.28.70

***Highlights**

> Original and new experimental fire tests within a 20 m cubic atrium.

> Simulations with FDSv5.3.3 validated experimentally.

> Physical or non-physical nature of the numerical results depending on the modelling of the make-up inlet air.

On the Fluid Dynamics of the Make-Up Inlet Air and the Prediction of Anomalous Fire Dynamics in a Large-Scale Facility

Cándido Gutiérrez-Montes[a,*], Enrique Sanmiguel-Rojas[a], Manuel A. Burgos[b], Antonio Viedma[b]

[a]Fluid Dynamics Division of the Department of Mechanical and Mining Engineering, University of Jaen, Jaen, Spain

[b]Department of Thermal and Fluid Engineering, Technical University of Cartagena, Murcia, Spain

*Corresponding author: Tel.: +34953212903; fax: +34953212870.

E-mail address: cgmontes@ujaen.es (C. Gutiérrez-Montes)

Postal address: Despacho 022/023, Área de Mecánica de Fluidos, Departamento de Ingeniería Mecánica y Minera, Edificio A3, Campus Las Lagunillas, 23009, Jaén, España.

Abstract:

The present paper is focused on the fluid dynamics of the make-up air at the vents in case of an atrium fire, its influence on the fire-induced conditions and the necessity of properly model it to obtain an accurate numerical prediction. For this aim, experimental data from two full-scale atrium fire tests conducted in a 20 m cubic facility, with venting conditions involving mechanical smoke exhaust and make-up air velocities larger than 1 m/s, and with different fire powers, are presented. Subsequent numerical

simulations of these tests have been performed with the code Fire Dynamics Simulator v5.5.3. Two different approaches have been followed to simulate the make-up air inlet fluid dynamics, involving one domain which only considers the inside of the building and another which includes part of the outside. In the former simulations, anomalous phenomena around the fire appear, while the inclusion of the exterior domain provides with a completely different fluid dynamics inside the facility which agrees better with the experimental data. A detailed analysis of the fluid mechanics at the air inlet vents is conducted to explain these discrepancies. Finally, further simulations are performed varying the make-up area to assess the appearance of the aforementioned phenomenon.

Keywords: make-up air, mechanical exhaust, CFD simulations, atrium, full-scale fire tests.

1. Introduction

One of the most challenging tasks for a fire engineer is the accurate computation of the fire-induced conditions within a large enclosure, such as an atrium, in the design process of a comprehensive fire protection system. Furthermore, this issue constitutes one of the active ongoing research topics within the fire research community [1].

At this point, there is still a large uncertainty on the necessary inlet conditions of the make-up inlet air, in order not to severely influence the inner fire-induced conditions, by perturbing the flame, the plume, the smoke movement or the smoke layer formation and growth, and, thus, endangering even more the lives of the building occupants. This uncertainty, has led the current fire-safety codes to be very restrictive on this matter,

which demand numerous goals [2] to be accomplished by the make-up air supply system, such as to be uncontaminated outdoor air or to be supplied from positions below the smoke layer and at low velocity [3], not to disturb the flame and plume. The no fulfilment of these requirements could cause a faulty performance of the fire protection system, specifically of the smoke management system.

Regarding the make-up air inlet velocity, the majority of the current codes [4, 5] establish a maximum velocity of 1 m/s, in order not to negatively affect the inner conditions in case of fire. However, in these standards, there is a provision for a modification of the maximum inlet velocity if this is supported by engineering analyses, being ones of the most common studies those from computational fluid dynamics (CFD) modelling, widely used in the study of smoke movement phenomena [6] or of fire propagation [7].

The use of these engineering tools is of great importance and value as they allow design complex fire-protection systems and optimize them within enclosures that are not considered in the aforementioned standards and codes. The development of these codes has also permitted the implementation of new regulations [8] supported by performance-based and risk-informed studies, very important when considering atria. Nevertheless, as it has been mentioned before, the study of the fire-induced conditions within atria constitutes an ongoing research topic and, specifically regarding the CFD models, there is a need to conduct further validation and verification studies [9-13] in order to continue filling the existing gaps of knowledge, assess the right use of these models and set bounds to their range of applicability, in the look for a reliable and accurate tool that lead to the achievement of fire-safe real designs.

In the recent years, some researchers have dealt with this make-up air issue, such as the studies from Hadjisophocleous and Lougheed [14], Yi et al. [15] or Kerber and Milke [16] on the influence of the vents location and arrangement, as well as inlet velocities, on the fire-induced conditions. These works were conducted considering different shaped and sized atria and gave guidance on these matters, finding advisable to supply the fresh air below the theoretical smoke layer height, within a symmetric venting topology and at velocities lower than 1 m/s, to avoid plume perturbations, which reinforced the requirements and goals of the abovementioned fire codes. Furthermore, it was also suggested that the inlet velocities should be diffused so that they were very low when they reached the fire and had no effect on it.

More recently, detailed studies considering the influence of the air velocity [17] or the outer wind [18] on the inner fire-induced conditions within atria have been also conducted. In these works, it has been also found that make-up air inlet velocities larger than 1 m/s, or even lower, can disturb the plume, enhancing the mass interchange at the smoke layer interface and resulting in a lower smoke layer interface. This effect was noticed to be stronger for atria heights below 20 m.

The performance of these studies has reported a considerable amount of valuable information and has contributed to enrich the state-of-the-art on this matter. However, not all the studies reported in the technical literature, or the existing engineering designs, are properly validated and verified with experimental data or by means of numerical tests, such as grid sensitivity or domain extension studies. At this point, and regarding the numerical tests, Zhang et al. [19] have studied the necessity of including

part of the exterior domain to proper simulate a small enclosure fire, such as the one from Steckler et al. [20]. In addition, in a recent work [12] three different make-up air inlet conditions were both, experimentally and numerically, assessed in case of an atrium fire, including make-up air velocities of the order of 1 m/s. It was found that, while in the experiments no significant variations were observed on the fire-induced conditions, there were discrepancies between the predicted results when relatively high inlet velocities were considered.

The present work reports full-scale experimental data of two atrium fire tests. The two tests were conducted as part of the Murcia Atrium Fire Tests [10-12]. In both tests, the same venting conditions were considered, with make-up velocities larger than 1 m/s, only varying the fire power. Detailed transient measurements of gas temperatures, as well as airflow at the inlets are reported. Later CFD simulations of these tests have been performed using the code Fire Dynamics Simulator version 5.5.3 (FDSv5.5.3), considering two different computational domains, in order to compare the predictions with the experiments, check its capability to properly predict the fire-induced conditions and explain the discrepancies observed in [12]. For this aim, special attention is paid on the fluid dynamics conditions at the inlet vents. Section 2 is devoted to describe the experimental facility and tests conditions, as well as the numerical model and the computational domains considered. In §3, a comparison between the experimental measurements and the numerical predictions, for the two tests, is conducted and discussed. §4 is devoted to explain the discrepancies between the numerical simulations and the experimental measurements showed in §3. Finally, the conclusions are included in §5.

2. Experimental tests and numerical model

- **Experiments:**

In this work, results from two different full-scale fire tests are presented. The experiments were conducted at the Fire Atrium of the Centro Tecnológico del Metal, Spain [10-12], as part of the Murcia Atrium Fire Tests. This facility, of 19.5 m x 19.5 x 19.5 m and pyramidal shaped roof, is made of 6 mm thick steel sheets and contains four exhaust fans, of nominal flow rate of 3.8 m^3/s, installed at the roof and eight make-up vents, of area 4.88 m x 2.5 m, arranged at the lower parts. A sketch and main dimensions of the Fire Atrium are showed in Figure 1 a.

The facility was implemented with sensors distributed at different key parts, summing a total of 61. The variables measured were the inner air temperature next to the walls, the make-up air temperature and velocity, the temperature at a central vertical section and the smoke through the fans temperature. A sketch of the main sensors and their approximate location is showed in Figure 1 b (the make-up air inlet conditions were measured at the centre of the vent). In addition, the weather conditions were measured, monitoring the temperature, humidity and pressure outside. For further details on the experimental set up see [10-12].

The burning fuel was heptane contained in a pool-fire located at the centre of the atrium floor, of 0.92 m diameter, in test #1 [12], and of 1.17 m diameter, in test #2. The venting conditions were the same for both tests, with the four fans activated and the make-up vents partially open at 2/9 of their area with symmetric layout, that is, the two vents at

the corners of the wall A (front wall) and the two vents of the wall C (back wall), with a total inlet area of 10.83 m^2, see zoomed area of Figure 1 a. In addition, a layer of water was added at the bottom of the pool-fire in order to insulate the metal from the burning pool heat, thus providing a more stable steady burning regime. The volume of water was checked to remain the same after the tests. A summary of the laboratory and ambient conditions during the tests is presented in table 1.

The heat release rate (HRR), $\dot{Q}$, of each test has been calculated as,

$$\dot{Q}(t) = \dot{m}(t)\chi_{eff}\Delta H_c, \quad (1)$$

where $\dot{m}(t)$ is the mass loss rate of the fuel, ΔH_c is the heat of combustion (44.6 MJ/kg [21]) and χ_{eff} the combustion efficiency (0.85±0.12 [22-24]). Figure 2 shows the HRR of the tests.

An uncertainty analysis for the measurements was conducted in [10, 11] showing a maximum total experimental uncertainty of 1.5% for the temperature, of 4% for the velocity probes and of 1 % for the fuel mass loss rate. The uncertainty associated with the HRR is estimated to be around ±15%. A detailed explanation of these calculations is presented in [11].

- **Numerical model:**

To simulate the experiments, the finite differences based code Fire Dynamics Simulator version 5 (FDSv5) [25] has been used. The heptane combustion has been simulated by

means of a mixture fraction combustion model. The measured HRR, Figure 2, has been set as an input. To take into account the turbulence, a large-eddy simulation (LES) approach [26] has been used. The radiative heat transfer is computed by solving the radiation transport equation for a non-scattering grey gas, and a value of 0.35 [27] has been set for the radiative fraction of the heptane pool-fire. The fans have been simulated by setting their nominal exhaust flow rate, and the vents as openings to the atmosphere. Finally, the walls and roof have been modelled as 6 mm thick steel sheets and the floor as a thick layer of concrete [28]. For further details see [11, 12].

Two different computational domains have been considered, Figure 3. Both domains include the atrium space, the walls and the roof, although the exterior domain has been considered only in one of them (domain #2). Different additional exterior lengths of outer domain have been considered, specifically 2.4 m and 3.25 m, although only the results for the last are presented here as no difference between both lengths has been noticed. A grid sensitivity study was conducted in [11, 12] which showed that a cell length of 0.13 m (grid size of 150 cells per side in case of domain #1), was fine enough to properly predict the fire-induced conditions. This grid size constitutes a value of the grid spatial resolution [22, 25], R^*, of ~ 1/8, for test #1, and ~ 1/10, for test #2. Furthermore, to assure grid independence, a grid size of 0.11 m (grid size of 180 cells per side in case of domain #1, ≈ 5.8 million cells) has been finally used (R^*, of ~ 1/10, for test #1, and ~ 1/12, for test #2). The same cell size has been used for both domains, thus for domain #2 a grid of 13.8 million cells has been used.

For the present work, parallel computing technique has been used, dividing each of the computational domains considered into 9 (multiple) meshes. However, in order to

assure that no spurious numerical solutions are obtained due to the parallel calculations, previous simulations of the two tests have been conducted using only one mesh, finding exactly the same behaviours reported in the present work. These simulations have been also conducted for different spatial resolutions, specifically grids of 90 x 90 x 90 cells, 150 x 150 x 150 cells and 180 x 180 x 180 cells have been used.

3. Results

In the present section, a comparison between the transient experimental measurements and the numerical predictions, for the two tests is conducted and discussed. The experimental data are compared with the numerical simulations for both domains and for all the sensors of Figure 1 b, that is, the centreline temperature (ideally the plume), the smoke through the fans temperature, the air close to walls temperature and the make-up air inlet velocity at the vents. In addition, by means of the N - percent method [10, 11, 15, 29], the smoke layer height has been also considered. Measurements - time evolutions at different locations are presented for test #1, in table 2, and test #2, in table 3.

- Test #1:

The test #1 was with the four fans activated, the vents partially open, with a total inlet area of 10.83 m^2, and the pool-fire of 0.92 m diameter, with a fire power of 1.22 MW. Figures 4 and 5 show the comparisons between the measurements and the numerical predictions.

In test #1, the experimental fire-induced conditions evolved normally, without any noticeable phenomenon taking part in it. Following the figure sequence Figure 4 a, c, g and e, Figure 5 a, c, and e, it can be observed how the centreline temperature starts first to rise at the location closest to the flame, h = 5.25 m, sensor 25, and, consecutively, at h = 9.25 m, sensor 27, h = 13.25 m, sensor 29, and, finally, at the exhaust fans region, sensors 59 and 60, indicating the formation of the fire plume. At the upper locations of the centreline, the smoke temperature shows a progressive and continuous rise due to the smoke accumulation and the formation and growth of the smoke layer, first at the fans region and, then, at h = 13.25 m. The smoke-layer growth can be also deduced from the temperature rise at the near the walls region, sensors 1, 4, 7, 12, 16 and 19. Contrary to the central parts, the temperature rises first at the highest location, h = 15 m, sensors 1 and 12, as the smoke layer reaches first this region. Again, a continuous temperature rise is observed without any sudden variation affecting the measurements. At the final stages of the fire, at the upper locations, above h = 10 m, almost a constant temperature is reached, indicating that quasi-steady fire-induced conditions were being reached. Only the temperature at h = 5 m near the walls, sensors 7 and 16, shows a small increase, which indicates that the smoke layer continued growing slowly near that region.

Regarding the comparison between the experimental data and the numerical results, on the left column, Figure 4 a, c, e and g and Figure 5 a, c, e, g and i, the experiment is compared with the simulation without the inclusion of part of the exterior domain (domain #1) and, on the right column, Figure 4 b, d, f and h and Figure 5 b, d, f, h and j, the experiment is compared with the results from the simulation with the inclusion of the exterior domain (domain #2), both for the same sensors' measurements. At the

centreline and at the fans region, both simulations evolve similarly for the first 200 - 250 s, approximately, that is, the fire plume forms and the temperature starts to rise fast, remaining more or less constant at the location closest to the fire, Figure 4 a and b, and rising progressively at the upper parts, above h = 10 m. However, from that moment, very different fire-induced conditions are predicted by the two simulations, above all at the lower parts. For the domain #1, after t = 250 s, a sudden temperature drop occurs, predicting temperature values much lower than those measured in the experiment. This sudden temperature drop or anomaly affects all the regions considered, e.g. it appears at t = 299 s at h = 5.25 m, at t = 311 s at h = 13.25 m or at t = 320 s at the fans region. These differences are larger at the locations closer to the fire, with maximum discrepancies, relative to the measurements, of 64 % at h = 5.25 m, 36 % at h = 9.25 m, and reduce with height, due to the larger plume diameter and the attenuation effect that the smoke layer has on this phenomenon, being the discrepancies equal to 26 % at h = 13.25 m, and of 27 % at the exhaust fans region at the end. On the other hand, for the domain #2, which includes part of the exterior, the fire evolved similarly to the experiment and good agreement is found at all the locations of the centreline, with no difference at all, and slightly underpredicting the smoke temperature at the fans regions, with a maximum difference of approximately 20 %. At the fans region, both simulations show almost the same predicted value, as a result of the before commented attenuation effect of the smoke layer on the phenomenon that appears in domain #1.

If now the close to the walls region is considered, similar trends are observed for both simulations at h = 15 and h = 10 m, slightly underpredicting the temperature at the end, with differences of 19 % (domain #1) and 16 % (domain #2) and of 17 % (domain #1) and 17 % (domain #2), respectively. However, if analyzed in detail, domain #1 presents

small sudden temperature variations due to the aforementioned phenomenon, e.g. at t = 330 s the smoke temperature stops rising at h = 15 m, remaining constant for 50 s, while the temperature keeps rising continuously at domain #2. These variations reflect a more chaotic fire-induced conditions' evolution for domain #1. Besides, at h = 5 m near the walls, at t = 354 s a sudden temperature rise occurs in domain #1, overpredicting the smoke temperature at that location by more than 49 %, being the agreement really good when the exterior domain is included, domain #2. In addition, if these three locations are put together, it can be appreciated that there is no thermal stratification in domain #1, contrary to what it has been measured experimentally, to which is expected to occur [21] and to what it has been obtained from domain #2.

This phenomenon on domain #1 also affects the smoke layer height evolution, Figure 5 g, where a no continuous evolution is observed, e.g. at t = 250 s. In addition, the predicted final smoke layer height is lower than the one predicted by the simulation with domain #2, Figure 5 h, which is also in good agreement with the experimentally calculated (N = 30 %).

Finally, Figure 5 i and j, shows the comparison of the make-up air inlet velocity at one of the vents. Relative good agreement is observed in both simulations, slightly being overpredicted the experimental measurements. The experimental data show more variable values due to the non-steady outdoors conditions, which have not been taken into account in none of the simulations. Regarding the two simulations, a more variable inlet velocity pattern is shown by the simulation with domain #1, possibly due to the stronger influence that the inner conditions have on the inlet ones, as will be later explained.

- Test #2:

Test #2 was with the same venting conditions as test #1, and the pool-fire of 1.17 m diameter, with a fire power of 2.06 MW. Figures 6 and 7 show the comparison between the experiment and the domain #1, on the left column, and between the experiment and the domain #2, on the right column, for the locations considered.

As in the test #1, the experimental fire-induced conditions evolved normally with no significant effect affecting them, Figure 8. Again, at the central region, the smoke temperature reaches fast a quasi-constant value at the location closest to the fire, sensor 25, while at the upper locations a continuous temperature rise is observed, due to the hot smoke from the plume accumulation. The fire-power of this test is sensibly larger than in test #1, almost 170 % larger, and, as the venting and atmospheric conditions are quite similar, the temperatures reached all over the whole domain are higher. However, different from test #1, at the upper parts, the temperature shows a positive slope at the final stages of the fire, which indicates that the fire-induced conditions were still evolving, that the smoke layer was still growing and, thus, that no steady-conditions had been reached yet. Finally, if the near the walls smoke temperature is analyzed, there is a clear thermal stratification, in which the upper parts, h = 15 and 10 m, show similar temperatures 109 ºC and 105 ºC, respectively, while at h = 5 m, the temperature at the final stages is around 60 ºC. These temperature values also reflect the proximity of the smoke layer interface to the last location, as shown in Figure 7 g and h (N = 30 %).

Regarding the numerical simulations, similar trends to those of test #1 are observed for test #2. During the first instants, before t = 250 s, both simulations evolved similarly, that is, a vertical smoke plume formed, e.g. in domain #1, Figure 9 a and b, and the hot smoke reaching the ceiling started to accumulate, building up the smoke layer. However, from t = 250 s, approximately, really different fire-induced conditions are predicted by the two simulations. As happened in test #1, the simulation with domain #1 predicts a sudden temperate drop at the central section, which affects the whole domain. This temperature drop remains permanent until the end of the simulation and is due to a flame lean, and the subsequent plume deviation, Figure 9 c and d. On the contrary, for the simulation with domain #2, the flame remained almost vertical during the whole simulation and, thus, did the smoke plume. These kinds of flame leans are normal within fires, as these are non-steady, chaotic and unstable phenomena, although, under the fire test conditions simulated and taking into account the experiment conducted, the possible flame inclinations, Figure 8, do not affect in such way the fire induced conditions. As a consequence of the above commented events, again the centreline temperature is underpredicted with maximum discrepancies of 75 %, at h = 5.25 m, 42 %, at h = 9.25 m, and 36 %, at h = 13.25 m, in domain #1, while really good agreement is achieved in domain #2. As happened in test #1, the smoke layer attenuates the possible impact of these flame inclinations over the upper and far from the fire locations. This provokes that, although there is certain influence at these parts, e.g. at t = 370 s at the fans region, Figure 6 g and h, quite similar results are obtained at these upper levels for both simulations, as the fire power, which is the same for both cases, is prescribed as an input and the make-up air intake remains similar in both cases. Therefore, the smoke temperature is slightly underpredicted at this zone with differences of 19 and 17 %, at the fans, 13 and 14 %, at h = 15 m near the walls, and 11

and 14 %, at h = 10 m near the walls, within the accuracy associated to the code, for domain #1 and domain #2, respectively, at the end. The main differences between both simulations at the far field appear, as in test #1, at the lower parts, that is, at h = 5 m, Figure 7 e and f. At this location, a sudden temperature increase occurs in domain #1, whereas the temperature rises progressively in domain #2, as a consequence of the smoke layer growth. This sudden temperature rise observed in domain #1 provokes the temperature reached at this height to be almost identical to the one at h = 10 m, thus not predicting any thermal smoke layer stratification, contrary to what it is predicted by the simulation with domain #2. At the end, the temperature at this location is overpredicted by more than 61 %, domain #1, and 27 %, domain #2. These anomalies are also reflected at the smoke layer evolution, which grows continuously in domain #2, in perfect agreement with the experiments (N = 30 %), whereas domain #1 presents a non-continuous evolution, e.g. at t = 360 s, being also predicted a final smoke layer height sensibly lower than the one from the experiment. Finally, as in test #1, quite good agreement is obtained between both simulations and the experiments for the make-up air inlet velocities.

4. Discussion. Discrepancies between the numerical simulations

In the present section, the previous results will be commented and discussed in order to find an explanation for the discrepancies observed between the different simulations of test #1 and test #2. As it has been commented before, some works [12, 16-18] have shown that make-up air velocities of the order or larger than 1 m/s can disturb considerably both the fire and plume and, thus, can have a significant influence on the fire-induced conditions. However, in a previous work [12], different venting conditions

were analyzed, including make-up velocities larger than 1 m/s, not finding any significant influence of these velocities on the inner conditions' evolution, for the specific cases studied. In addition, in the previous section, it has been shown that, for the simulated tests, there are significant differences when the exterior domain is or is not included. These discrepancies are caused by an anomaly that appears when the exterior domain is not included, domain #1, which consists of the formation of a circular air stream surrounding the flame [12], which appears in the early stages of the simulation and which increases in intensity with time, Figures 9 and 10.

Figure 9 shows the velocity contours in a horizontal section at the central part of the vent for different times for domain #1, on the left column, and for domain #2, on the right column, for test #1. Both simulations start equally, with the formation of an inlet flow of fresh air incoming from the outside through each vent, e.g. Figure 9 a and b. As commented in the previous section, from t = 200 - 250 s, differences between both simulations start to appear. At that time, Figure 9 c and d, a light circular stream starts to form in domain #1, due to the perturbations induced by the typical flame movements. These flame inclinations are predicted by both simulations, although have only a significant effect on domain #1. As for domain #2, no effect is observed affecting the make-up air inlet. This current predicted in the simulation with domain #1 grows in intensity with time, which induces azimuthal velocities of 2 m/s surrounding the flame at, e.g., t = 445.3 s and which affects considerably the flame verticality, Figure 11 a and d. These azimuthal velocities rise up to values of 2.5 m/s at, e.g., t = 730.8 s, Figure 11 b and e, reaching a maximum value of 3.5 m/s at, e.g., t = 1062.3 s, Figure 11 c and f. On the other hand, the simulation with domain #2 evolves without the formation of any permanent circular stream around the flame during the whole fire. The effects of this

current, in domain #1, on the flame and on the predicted thermal field have been already presented in the previous section. In addition, the rapid air, flame and plume movement enhance the smoke mixing with the fresh air of the lower parts. This provokes that the smoke layer grows considerably, thus, being deeper than the one predicted by the simulation with domain #2 and, also, than the one obtained experimentally. Besides, this strong air movement affects, to a lesser extent, the upper parts, provoking the smoke mixing of all the sublayers and homogenizing the temperature of the whole smoke layer. This effect finds its minimum at the top of the facility. Figure 10, shows the same phenomena for test #2, where similar evolution and velocity values are observed, thus, showing no dependence of this effect on the fire power, for the cases studied.

The explanation for these discrepancies between both numerical simulations can be found, thus, focusing on the fluid dynamics at the inlet vent boundary conditions. Figure 12 shows qualitatively different flow patterns, that is, while in domain #1, a quite uniform inlet flow is predicted, in domain #2, a sudden contraction flow pattern is predicted, where a vena contracta forms. Figure 13 shows quantitative details of the velocity module and the x and y velocity components profiles for both simulations at the inlet vent, and for different lengths from the vents inside the facility, for different times at the early stages of the fire simulation, for test #1. At t = 50 s, when no inner circular air stream has formed yet in domain #1, similar velocity profiles are predicted by both simulations at the vent.

Furthermore, the y-component profile of both streams is even more similar. The largest difference lies in the x-component, which in the simulation with domain #1 is

practically null, regarding that the conditions at the vent have been fixed to be those of a quiescent atmosphere at ambient pressure, whereas in the simulation with domain #2, these conditions have been set far away from the inlet vent, letting the flow evolve freely and only as a consequence of the inner induced conditions.

In addition, in domain #1, the inlet air flow velocity profiles remain invariable with the distance in the vicinity of the vent, and in domain #2 the y-component of the velocity increases due to the vena contracta effect, turning into a parabolic-profile flow, thus, increasing the y-momentum of the inlet flow. In the case of domain #1, the absence of transverse velocity component, and regarding the condition at the vents remain constant, the flow is highly sensitive to any transverse variation that can appear inside the domain.

As it has been previously commented, the numerical predictions obtained are not spurious solutions but a direct consequence of how the make-up air inlet flow field is modelled in each domain. All these phenomena affecting the simulation with domain #1 are due to the fact that, when the open boundary condition is used in FDS, the flow inlet conditions are computed assuming ideal flow, that is, inviscid, steady and incompressible flow, by means of the Bernouilli equation as,

$$p_1 + \frac{1}{2}\rho_1 v_1^2 + \rho_1 g z_1 = p_2 + \frac{1}{2}\rho_2 v_2^2 + \rho_2 g z_2 \,, \tag{2}$$

being p the static pressure, ρ the flow density, v the flow velocity, g the gravity acceleration modulus and z the vertical height, and the subscripts 1 and 2 refer to the conditions upstream and downstream, respectively. In this case, there is no variation on the potential energy term and the conditions at the upstream flow are set as an input, being the pressure equal to the atmospheric one and the velocity equal to zero.

Therefore, the downstream velocity is just a function of the pressure difference and the downstream density, which is the case of domain #1 for the inlet velocity computation at the vent. This fact explains the null x-component velocity and the quasi-uniform y-velocity profile at the vent in the simulation with domain #1 in the early stages. It has to be also taken into account that, when this boundary condition is used, only the velocity module is imposed while the inlet direction is not fixed. In this way, once the inner perturbations induced by the fire travel upstream towards the vents, they affect the inlet currents and deflect them, and the flow velocity is not able to recover the normal direction to the inlet boundary again. This numerical phenomenon has a feedback nature with catastrophic effects in the simulations. On the other hand, when part of the exterior domain is included as computational domain, the inlet velocity of the outer cells at the boundaries is computed as explained before, however, at the rest of the inside computational domain, the flow evolves fulfilling the Navier-Stokes equations [25]. It can be observed from the last row of Figure 13 that, in this case, the current is always normal to the boundary, and the simulation of the whole vent has a bottleneck effect, which prevents the inner instabilities travelling upstream towards the outer computational domain and disturbing the outer Bernouilli boundary condition.

However, it is well known that the inclusion of part of the exterior domain involves larger computational requirements and computing times to achieve an accurate solution. In our case the time computing ratio, domain #2 vs domain #1, was 1.74, approximately. The abovementioned phenomenon has been observed for the particular experimental cases studied, although not such an effect has been observed for other experimental cases, and subsequent simulations, for similar fire-powers but lower inlet air velocities [11, 12]. In both tests, the venting conditions were the same with induced

make-up air inlet velocities larger than 1 m/s. Next, simply to show the appearance of the aforementioned anomaly for the specific case of test #1 and to observe when the inclusion of an exterior domain is necessary for a proper fire-induced conditions prediction, the numerical results for test #1 for different make-up air inlet areas with symmetric venting topology are presented. Specifically, the vents have been partially open at 1/2, 1/3, 2.5/9, and 1/9 of their total inlet area, that is, with a total inlet area of 24.375 m^2, 16.25 m^2, 13.541667 m^2 and 5.41667 m^2, respectively. Table 4 presents the average velocity values at the vents for both simulations, and Figure 15 shows the velocity contours predicted by the simulation with domain #1, on the left column, by the simulation with domain #2, on the right column, at the half part of the fire simulation, and the comparison of the predicted temporal temperature evolutions at three key locations inside the facility, at the central column. For the cases simulated, it can be observed that almost identical temperatures are predicted for the first two cases, with make-up air inlet velocities up to 1 m/s, being the velocity contours also quite similar. However, for the last two cases, with inlet velocities larger than, approximately, 1 m/s, the no inclusion of part of the exterior domain provokes the formation for a non-physical circular air stream around the flame that perturbs the fire-induced inner conditions, Figure 15 h and k, homogenizing the smoke layer temperature and enhancing the lower-fresh air mixing with the smoke layer. However, it has to be taken into account that these observations are only valid for the specific cases considered in this part.

6 Conclusions

It has been found in the technical bibliography that many of the studies conducted on the venting conditions in case of atrium fires only consider the inside of the facility. Many conclusions have been drawn from these works and also many building designs have been conducted under these considerations. In the present paper, the anomaly found in a previous work [12] has been analyzed and explained. For this aim, experimental results from two full-scale fire tests with symmetric venting topology, make-up air inlet area of 10.83 m^2, and different fire powers, 1.22 and 2.06 MW, have been reported. Later, FDSv5.5.3 simulations of these tests have been conducted considering two different computational domains, one which only includes the inside of the facility, domain #1, and another one which considers also part of the outside, domain #2. In order to rule out artificial numerical results due to the parallel computation, the results have been previously checked performing simulations of the tests considering only one mesh (no parallel computation).

From the simulations, quite different fire-induced conditions have been obtained. When only the interior is considered, a non-physical circular stream surrounding the flame forms, while this phenomenon is not predicted for the case in which part of the exterior domain is taken into account, and which also agrees much better with the experimental data. This effect has been obtained for both fire powers and, thus, under the fire conditions studied, no dependence on this parameter has been observed. The fluid dynamics at the vents entrance has been analyzed finding different inlet velocity patterns induced by the Bernouilli equation use at the inlet, domain #1, or the resolution of the proper Navier-Stokes equations at the vents, domain #2. This effect has been only reported for the specific venting conditions of the fire tests studied, with make-up air inlet velocities larger than 1 m/s, but has not been observed in other studied cases [11,

12]. Finally, the comparison of both domains has been extended for test #1 for different make-up air inlet areas, remaining the rest of the parameters unchanged. The inlet areas considered have been 24.375 m^2, 16.25 m^2, 13.541667 m^2 and 5.41667 m^2, respectively. It has been observed that, for the cases studied here, significant differences appear for inlet velocities larger than 1 m/s.

The results from this work can be only applied to the specific cases studied and a more extensive studied would be necessary to assess the appearance of the anomalies here reported. This study should consider parameters such as the vents location, the inlet vent velocity, the transversal inlet vent length, the distance to the fire or additional fire powers, not included in the present paper. In any case, not only a grid sensitivity study should be performed when conducting a design or study of the fire-induced conditions within a building with similar characteristics to the one presented in this work but also, the fire engineer or fire researcher will have to take into account the possible effects of an inappropriate set of the boundary conditions.

Acknowledgements

This research was supported by the Spanish MCyT and Junta de Andalucia under Projects # DPI2008-06624-C03-02 and # P07-TEP02693, respectively. CGM wants to acknowledge the research stay grants IAC-2010-3 and A-13-2010 from the Junta de Andalucia and the University of Jaén, respectively.

References

[1] Gutiérrez-Montes, C., Rein, G., Sanmiguel-Rojas, E., Viedma, A. Smoke and fire dynamics in atria and large enclosures: an overview (Chapter 1 - Fire Safety), Nova Science Publishers, New York, 2009.

[2] Duda, S. Atria smoke exhaust: 3 approaches to replacement air delivery. ASHRAE Journal, 46(6): 21-27, 2004 (Atlanta, GA).

[3] Klote, J.H.; Milke, J.A. Design of smoke management system; ASHRAE Inc.: Atlanta, GA, USA, 2002.

[4] NFPA 92B. Standard for Smoke Management Systems in Malls, Atria, and Large Areas. National Fire Protection Association: Quincy, MA, 2009.

[5] International Code Council. (2009). 2009 International Building Code. Country Club Hills, IL: International Code Council.

[6] McCartney, C.J.; Lougheed, G.D.; Weckman, E.J. CFD investigation of balcony spill plumes in atria. ASHRAE Transactions, 2008, 114(1), 369-378.

[7] Jahn, W., Rein, G., Torero, J.L.. A posteriori modelling of the growth phase of Dalmarnock Fire Test One. Building and Environment, 2011**,** 46**(5)**, 1065-1073**.**

[8] Wade, C., Beever, P., Fleischmann, C., Lester, J., Lloydd, D., Moule, A., Saunders, N., Thorby, P. Developing Fire Performance Criteria for New Zealand's Performance Based Building Code. ISO TC92; Fire Safety Engineering International Seminar: Paris, 2007. New York City Fire Code. 2009. International Code Council, NY, USA, 2009.

[9] Chow, W.K., Li, S.S., Gao, Y., Chow, C.L. Numerical studies on atrium smoke movement and control with validation by field tests. Building and Environment 44 (2009) 1150–1155

[10] Gutiérrez-Montes, C., Sanmiguel-Rojas, E., Kaiser, A.S., Viedma, A. Numerical model and validation experiments of atrium enclosure fire in a new fire test facility. Building and Environment 2008, 43(11), 1912–28.

[11] Gutiérrez-Montes, C., Sanmiguel-Rojas, E., Viedma, A., Rein, G. Experimental data and numerical modelling of 1.3 and 2.3MW fires in a 20 m cubic atrium. Building and Environment 2009, 44 (9), 1827–1839.

[12] Gutiérrez-Montes, C., Sanmiguel-Rojas, E., Viedma, A. Influence of different make-up air configurations on the fire-induced conditions in an atrium. Building and Environment, 2010, 45(11), 2458-2472

[13] McGrattan, K., McDermott, R., Hostikka, S., Floyd, J. Fire Dynamics Simulator (Version 5) Technical Reference Guide. Volume 3: Validation. NIST Special Publication 1018-5; National Institute of Standards and Technology, 2010.

[14] Hadjisophocleous, G.V.; Lougheed, G. Experimental and numerical study of smoke conditions in an atrium with mechanical exhaust. International Journal on Engineering Performance-Based Fire Codes, 1999, 1(3), 183–7.

[15] Yi, L.; Chow, W.K.; Li, Y.Z.; Huo, R. A simple two-layer zone model on mechanical exhaust in an atrium. Building and Environment, 2005, 40(7), 869–880.

[16] Kerber, S.; Milke, J.A. Using FDS to Simulate Smoke Layer Interface Height in a Simple Atrium, Fire Technology, 2007, 43, 45–75.

[17] Hadjisophocleous, G.V., Zhou J., Evaluation of Atrium Smoke Exhaust Make-up Air Velocity, ASHRAE Transactions, 2008, 114, Part 1, 147-155.

[18] Zhou J., Hadjisophocleous, G.V., Parameters Affecting Fire Plumes, ASHRAE Transactions, 2008, 114, Part 1, 140-146

[19] Zhang, X., Yang, M., WANG, J., He, Y. Effects of Computational Domain on Numerical Simulation of Building Fires, Journal of Fire Protection Engineering, 2010, 20(4), 225-251

[20] Steckler, K.D., Quintiere, J.G., Rinkinen, W.J. Flow Induced by Fire in a Compartment, NBSIR B2-2520, Washington, DC, National Bureau of Standards, 1982.

[21] SFPE of fire protection of engineering. 4th ed. Quincy, MA, USA: National Fire Protection Association; 2008.

[22] Dreisbach J, McGrattan K. Verification and validation of selected fire models for nuclear power plant applications. In: Fire dynamics simulator (FDS), NUREG-1824 final report, vol. 7. U.S. Nuclear Regulatory Commission, Office of Nuclear Regulatory Research; May 2007.

[23] Hostikka S, Kokkala M, Vaari J. Experimental study of the localized room fires. NFSC2 test series (VTT building technology) VTT research notes 2104; 2001.

[24] Tewarson A. Combustion efficiency and its radiative component. Fire Safety Journal 2004, 39, 131–41.

[25] McGrattan, K., Hostikka, S., Floyd, J., Baum, H., Rehm, R., Mell, W., McDermott, R., Fire Dynamics Simulator (Version 5) Technical Reference Guide. Volume 1: Mathematical Model. NIST Special Publication 1018-5; National Institute of Standards and Technology, 2010.

[26] Pope SB. Computations of turbulent combustion: progress and challenges. Proceedings of the Combustion Institute 1990, 23, 591–612.

[27] Hamins A, Klassen M, Gore J, Kashiwagi T. Estimate of flame radiance via single location measurement in liquid pool fires. Combustion and Flame 1991, 86, 223–8.

[28] Incropera FP, DeWitt DP. Fundamentals of heat and mass transfer. 4thed. John Wiley & Sons; 1996.

[29] Cooper LY, Harkleroad M, Quintiere J, Reinkinen W. An experimental study of upper hot layer stratification in full-scale multi-room fire scenarios. Journal of Heat and mass transfer 1982;104:741–9.

Figure captions

Figure 1.Sketch and main dimensions of the fire-test facility in a, original nomenclature and location of the main sensors considered in b. Temperature sensors in squares and velocity sensors in triangles

Figure 2. Fire-tests HRR.

Figure 3. Snapshot of the computational domain and grid used: domain #1 in a, and domain #2, with part of the outside, in b. View from Wall A.

Figure 4. Test #1 measurements and predictions for domain #1, left column, and for domain #2, right column. Temperature at the centreline at 5.25 m high, first row, 9.25 m high, second row, 13.25 m high, third row, and at the exhaust fans, last row. Measurements identified by sensor number according to Figure 1.

Figure 5. Test #1 measurements and predictions for domain #1, left column, and for domain #2, right column. Temperature near the walls at 15 m high, first row, 10 m high, second row, and 5 m high, third row. Smoke layer height, fourth row. Make-up air velocities at the vent A1, last row. Measurements identified by sensor number according to Figure 1.

Figure 6. Test #2 measurements and predictions for domain #1, left column, and for domain #2, right column. Temperature at the centreline at 5.25 m high, first row, 9.25 m

high, second row, 13.25 m high, third row, and at the exhaust fans, last row. Measurements identified by sensor number according to Figure 1.

Figure 7. Test #2 measurements and predictions for domain #1, left column, and for domain #2, right column. Temperature near the walls at 15 m high, first row, 10 m high, second row, and 5 m high, third row. Smoke layer height, fourth row. Make-up air velocities at the vent A1, last row. Measurements identified by sensor number according to Figure 1.

Figure 8. Snapshots of the flame, both vertical and leant, for different times of test #2. 115 s in a, 425 s in b, 610 s in c, and 800 s in d.

Figure 9. Snapshots of the soot density and flame prediction for test #2 and domain #1. Vertical flame and unperturbed plume at t = 150 s in a, slightly leant flame and deviated plume at t = 250 s in b, and leant flame and deviated plume at t = 350 s in c, and at t = 450 s in d. View from Wall A.

Figure 10. Velocity contours at a horizontal plane at 1.25 m high, for different instants of the simulation with domain #1, left column, and for the same times of the simulation with domain #2, right column. Test #1. View from Wall A.

Figure 11. Velocity contours at a horizontal plane at 1.25 m high, for different instants of the simulation with domain #1, left column, and for the same times of the simulation with domain #2, right column. Test #2. View from Wall A.

Figure 12. Detail of vector velocities at a central horizontal section at 1.25 m high in first row, and respective temporal images of the flame completely leant and the plume deviated in second row. Test #1, domain #1. View from Wall A.

Figure 13. Vertical detail view of the vector make-up air inlet velocity at the vent A1 for different times, t = 50 s, in a and d, t = 150 s, in b and e, and t = 250 s, in c and f, for domain #1, first row, and domain #2, second row. Test #1. View from top of Wall A.

Figure 14. Predicted inlet velocity module, left column, y-component velocity, central column, and x-component velocity, right column, profiles at different lengths inside the vents: y = 0 m, triangles (domain #1) and solid line (domain #2), y = 018 m, circles (domain #1) and dashed line (domain #2), y = 0.54 m, stars (domain #1) and dash-dot line (domain #2), and y = 0.87 m, diamonds (domain #1) and dotted line (domain #2). t = 50 s, first row, t = 150 s, second row, and t = 250 s, third row. Test #1.

Figure 15. Velocity contours at t = 530.6 s at h = 1.25 m for the simulation with domain #1, left column, and with domain #2, right column. Log-linear temperature predictions comparison, central column, at the centreline at h = 5.25 m high, in red, triangles (domain #1), solid line (domain #2), at the exhaust fans, in blue, circles (domain #1), dashed line (domain #2), and at the near the walls region at h = 5 m high, in green, stars (domain #1), dash-dot line (domain #2). Inlet vent area of 24.375 m^2 first row, 16.25 m^2 second row, 13.541667 m^2 third row, and 5.41667 m^2 last row. Test #1. View from Wall A.

Table1

Fire test	Pool diameter (m)	Volume of heptane (l)	Burning time (s)	Open vents	Fans on	Ambient Temp (ºC)	Pressure (mbar)	HRR (MW)
test #1	0.92	52	1094	A1, A3, C1, C2 22%	All	27.5	1007	1.22
test #2	1.17	75	931	A1, A3, C1, C2 22%	All	28.0	1003	2.06

Table 1. Summary of laboratory and ambient conditions during the fire tests.

Table2

Time	Sensor number												
(s)	25	27	29	59	60	1	4	7	12	16	19	50	53
0.0	28.3	32.0	32.5	32.9	32.5	31.9	30.3	28.5	32.6	30.8	29.1	0.7	0.9
56.5	51.9	41.4	38.6	35.7	40.4	32.9	30.2	28.8	33.7	30.8	29.3	0.7	1.5
115.9	76.3	49.1	46.0	41.6	48.6	36.8	30.9	29.4	38.5	31.5	30.3	0.7	1.1
175.1	89.0	54.4	51.1	47.7	55.5	42.1	34.0	30.4	44.0	34.4	31.4	0.8	1.4
232.2	102.0	60.5	56.3	52.3	61.6	47.2	38.4	31.6	49.0	38.2	32.6	0.9	0.7
287.2	117.4	65.4	59.7	57.0	65.7	51.8	42.5	32.9	53.5	42.2	33.6	0.2	1.0
346.0	121.9	69.0	63.8	61.6	68.4	56.2	47.3	34.4	58.1	48.3	35.1	0.7	0.9
402.8	119.5	71.9	65.3	64.9	71.7	59.3	52.4	35.7	61.8	54.2	36.3	0.8	1.1
461.2	127.6	75.9	68.1	68.4	76.9	63.0	55.9	37.1	65.4	58.5	37.5	1.1	1.2
520.0	144.3	82.4	74.3	72.5	78.7	66.7	59.5	38.6	68.4	62.3	38.7	1.3	1.5
578.7	133.3	81.6	75.1	74.5	78.4	68.7	62.6	40.0	70.7	66.7	39.8	1.1	0.9
635.4	128.4	82.4	76.1	76.1	80.9	70.4	65.3	41.4	72.8	69.7	40.8	1.1	1.3
692.1	127.6	84.9	77.2	78.2	84.2	72.2	67.5	42.2	75.1	71.7	41.5	1.2	1.3
748.8	130.4	86.5	79.6	79.5	84.6	73.7	68.9	42.5	76.7	73.5	41.8	0.9	1.0
805.6	130.9	87.7	79.2	80.1	83.9	74.7	70.3	42.6	77.4	74.9	42.0	1.2	1.5
862.1	127.2	87.7	78.6	80.6	84.2	75.2	71.1	42.5	78.1	76.4	42.0	0.6	1.2
920.3	128.4	87.3	79.0	81.1	85.7	76.1	71.9	42.9	79.4	77.2	42.1	0.8	1.0
977.1	130.9	89.0	79.8	82.1	86.7	77.1	72.8	43.4	80.1	78.0	42.6	0.6	1.2
1032.2	131.3	89.8	81.5	82.9	87.3	77.5	73.4	43.6	80.5	78.6	43.0	0.9	1.1
1089.5	125.2	89.4	81.5	83.2	86.0	78.1	74.1	43.3	80.7	79.1	42.9	0.9	0.7

Table 2. Time - measurements for different sensors in test #1. Temperature values in ºC and velocity values in m/s. See figure 1 for sensor labels.

Table3

Time	Sensor number												
(s)	25	27	29	59	60	1	4	7	12	16	19	50	53
0.0	49.5	36.1	30.8	32.3	33.2	28.5	27.2	26.6	29.1	28.4	27.5	0.7	0.6
46.8	122.3	54.8	45.2	42.0	45.3	32.5	27.7	27.4	33.0	28.9	28.2	0.5	1.3
97.8	212.6	74.7	59.9	51.5	58.0	39.6	30.5	28.6	40.1	31.0	29.4	1.3	1.2
146.0	254.5	88.1	71.2	61.0	67.5	47.5	34.9	30.4	48.0	35.6	31.0	1.3	1.0
195.3	273.6	98.3	80.9	70.1	75.8	55.7	41.9	32.5	56.1	42.6	33.1	1.1	1.3
242.1	288.3	109.3	89.0	77.4	83.9	63.2	48.0	34.7	63.3	51.0	35.2	1.0	1.2
291.0	291.9	113.8	94.4	83.4	89.6	70.1	54.4	37.3	70.3	58.5	37.5	1.6	1.6
339.9	293.2	117.4	98.5	87.7	92.2	76.2	61.7	39.9	75.9	64.7	39.6	1.0	1.6
390.6	281.4	119.9	102.6	93.6	96.8	81.6	68.4	42.6	80.2	71.1	42.0	2.3	0.7
441.2	279.7	126.0	107.7	98.8	103.7	86.0	73.5	45.0	85.2	76.8	44.3	1.1	2.0
489.7	292.8	132.5	111.0	102.4	107.6	90.2	77.9	47.0	88.9	81.5	45.8	1.2	1.4
539.0	299.3	133.3	113.4	105.5	110.3	93.2	81.8	48.6	91.7	84.9	47.3	1.2	1.4
589.3	300.5	135.7	116.3	108.4	111.3	96.5	85.6	50.3	94.2	88.2	48.7	1.8	1.5
637.2	263.9	132.1	115.7	110.8	112.1	99.0	88.2	51.8	96.6	91.7	49.7	0.9	0.8
686.8	282.6	134.9	116.9	111.3	114.1	100.7	90.7	53.4	99.2	94.6	50.7	2.0	1.8
735.8	339.1	143.1	121.8	114.2	117.1	101.7	92.4	54.6	100.8	97.2	51.5	1.7	2.0
784.8	372.1	150.8	127.6	118.0	120.6	103.7	94.4	55.9	103.0	99.1	52.7	1.9	0.8
833.3	373.3	151.6	127.4	119.8	122.4	106.1	96.7	57.1	105.3	101.8	53.7	1.0	0.8
882.1	357.8	150.8	128.0	120.8	123.4	108.1	99.2	58.8	107.7	104.4	55.5	1.7	0.9
932.0	307.0	144.3	125.3	119.3	120.0	108.9	100.7	59.8	109.0	105.9	56.6	2.1	1.6

Table 3. Time - measurements for different sensors in test #2. Temperature values in ºC and velocity values in m/s. See figure 1 for sensor labels.

Table4

Opening ratio	Inlet velocity domain #1	Inlet velocity domain #2
1/2	0.5 - 0.6	0.55 - 0.65
1/3	0.8 - 0.9	0.9 - 1.0
2.5/9	1.1 - 1.3	1.0 - 1.2
1/9	2.1 - 2.3	3.1 - 3.3

Table 4. Average inlet make-up air velocity predicted for different inlet vents area simulations.

Figure1_eps

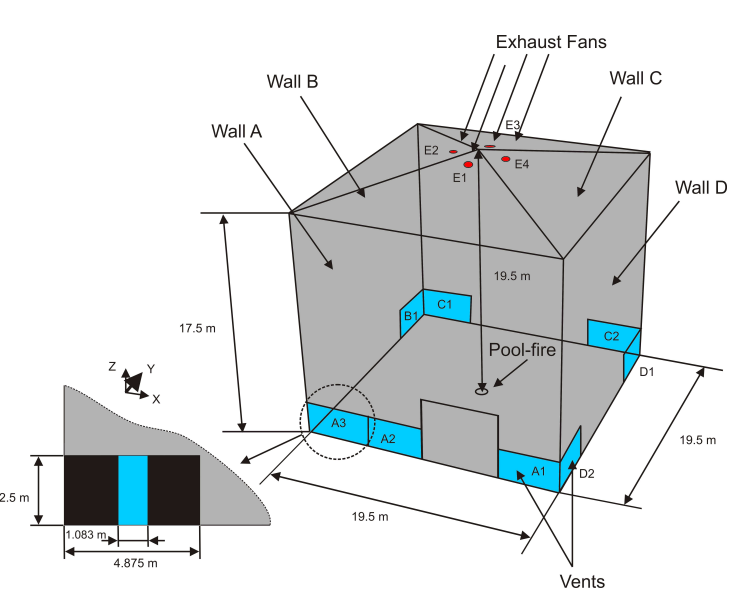
Exhaust Fans
Wall B
Wall C
Wall A
Wall D
E1
E2
E3
E4
19.5 m
17.5 m
B1
C1
C2
D1
D2
A1
A2
A3
Pool-fire
19.5 m
19.5 m
Z
Y
X
2.5 m
1.083 m
4.875 m
Vents

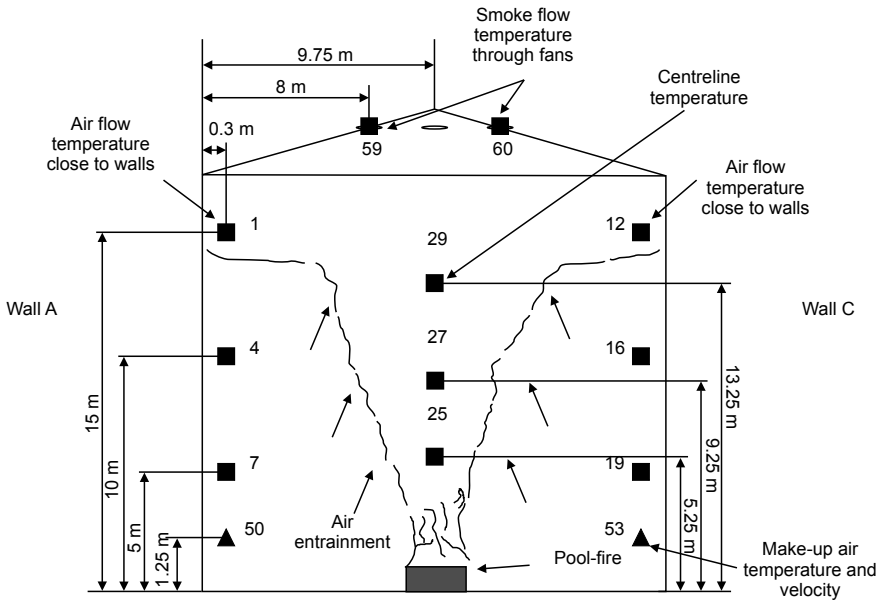
Smoke flow temperature through fans
9.75 m
8 m
Centreline temperature
Air flow temperature close to walls
0.3 m
59
60
Air flow temperature close to walls
1
12
29
Wall A
Wall C
4
27
16
15 m
13.25 m
25
10 m
7
19
9.25 m
5 m
50
Air entrainment
53
5.25 m
1.25 m
Pool-fire
Make-up air temperature and velocity

Figure2_eps

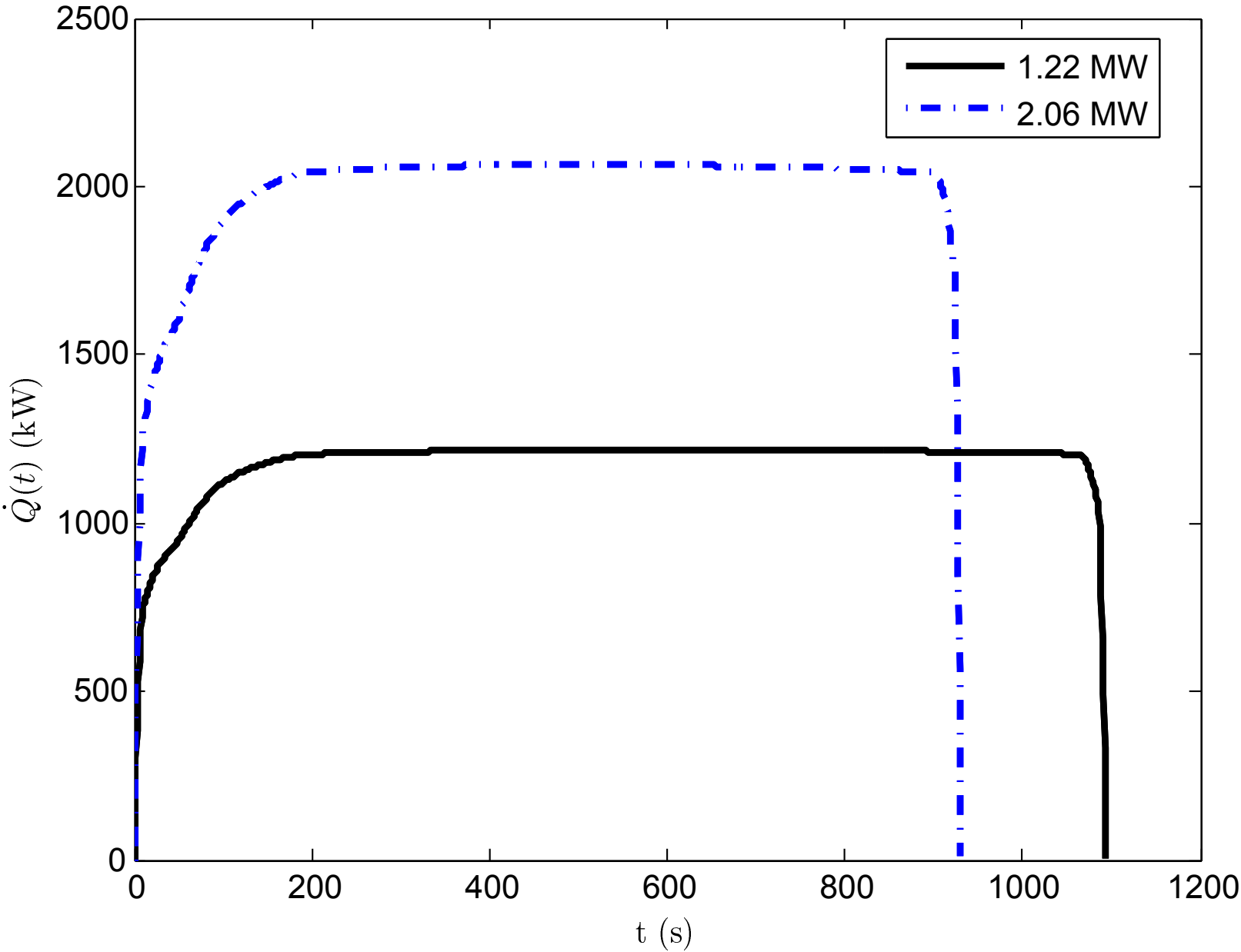
2500
2000
1500
1000
500
0
0
200
400
600
800
1000
1200
$\dot{Q}(t)$ (kW)
t (s)
1.22 MW
2.06 MW

Figure3_eps

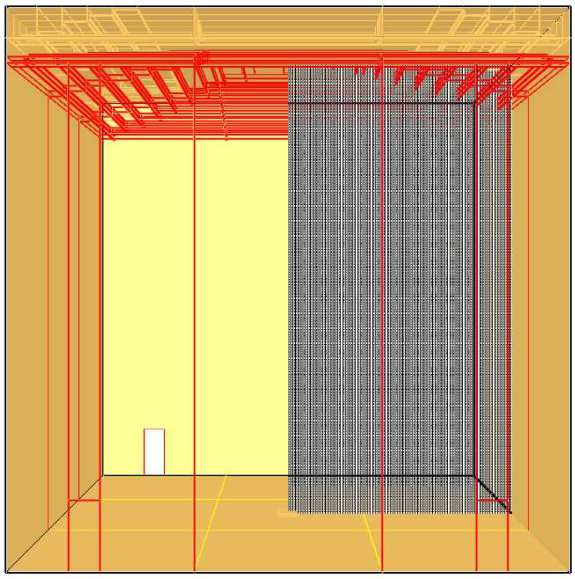

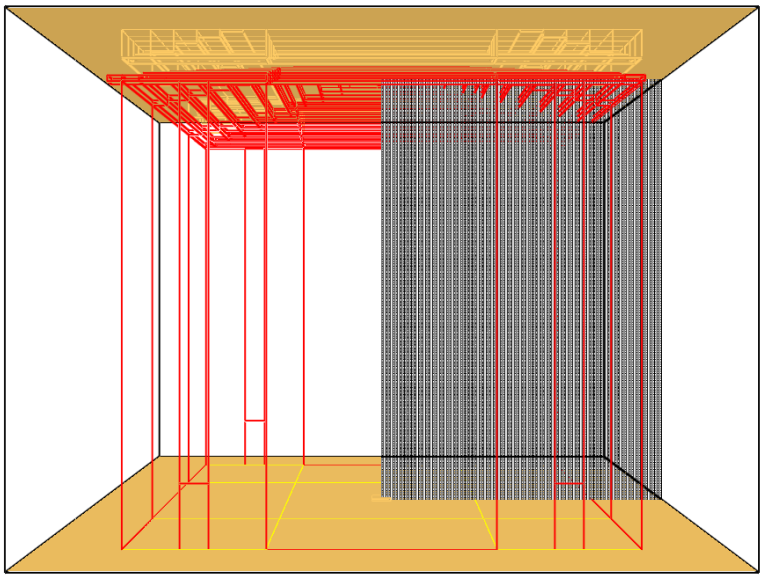

Figure4_eps

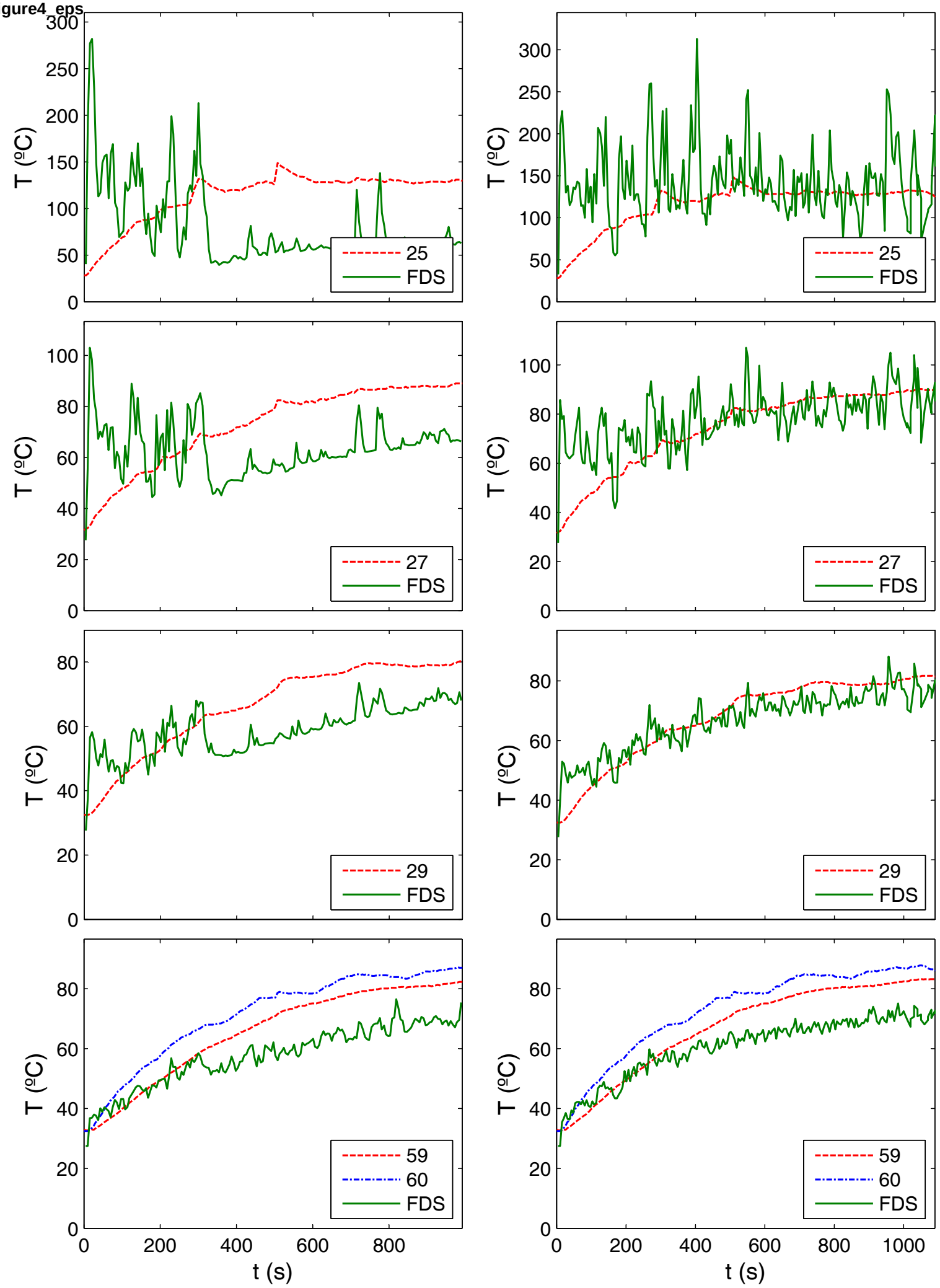

Figure5_eps

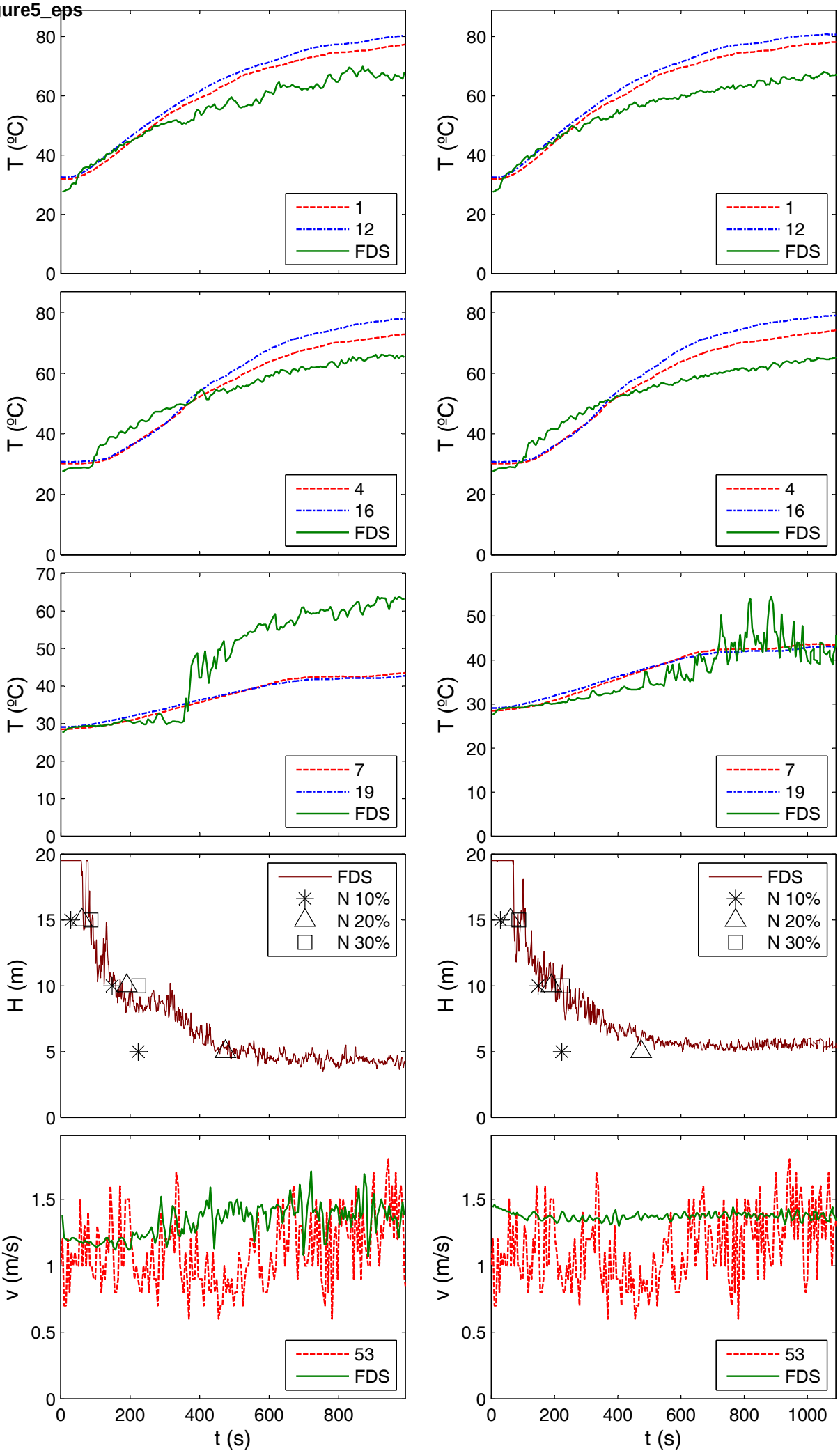

Figure6_eps

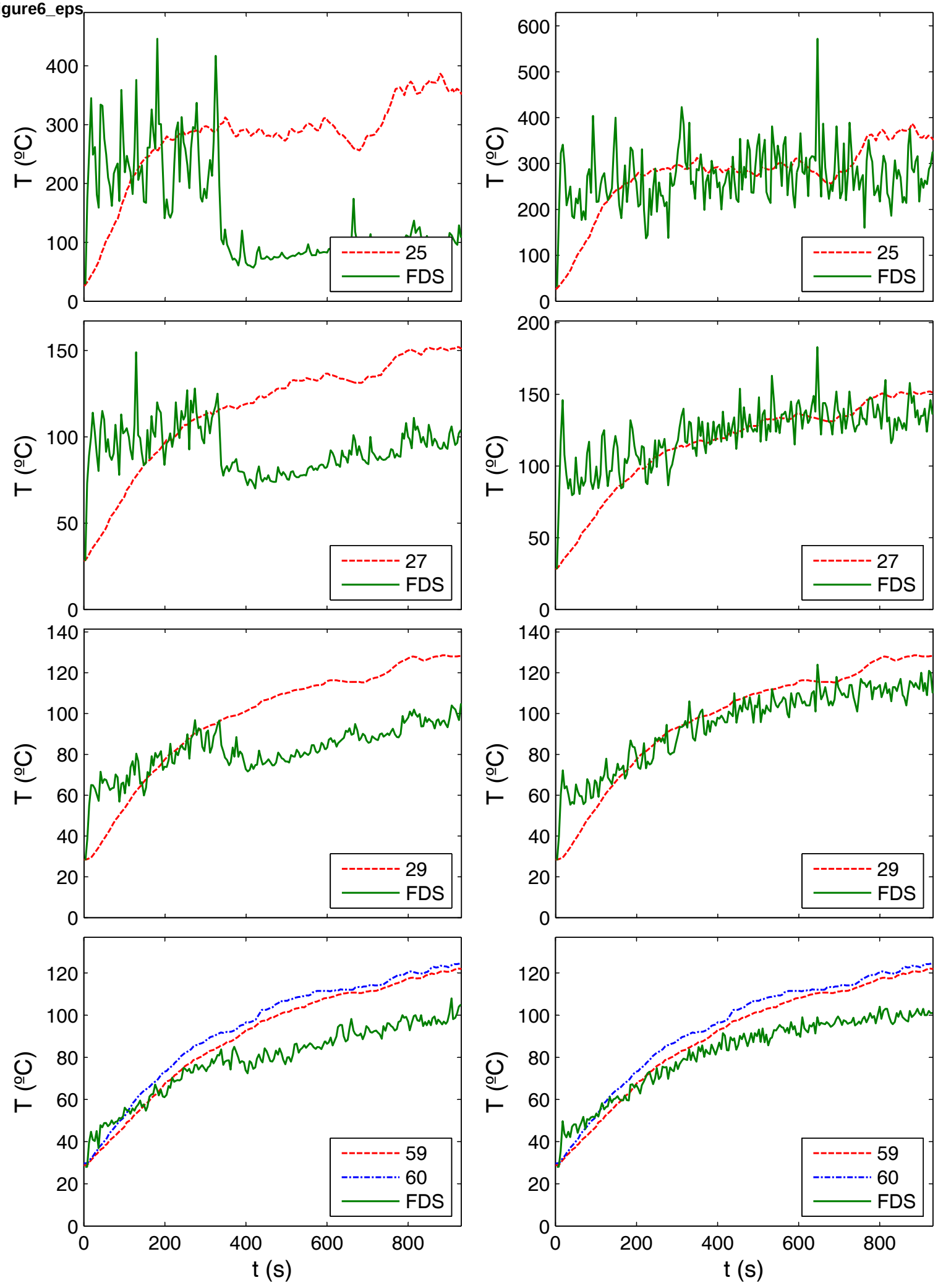

Figure7.eps

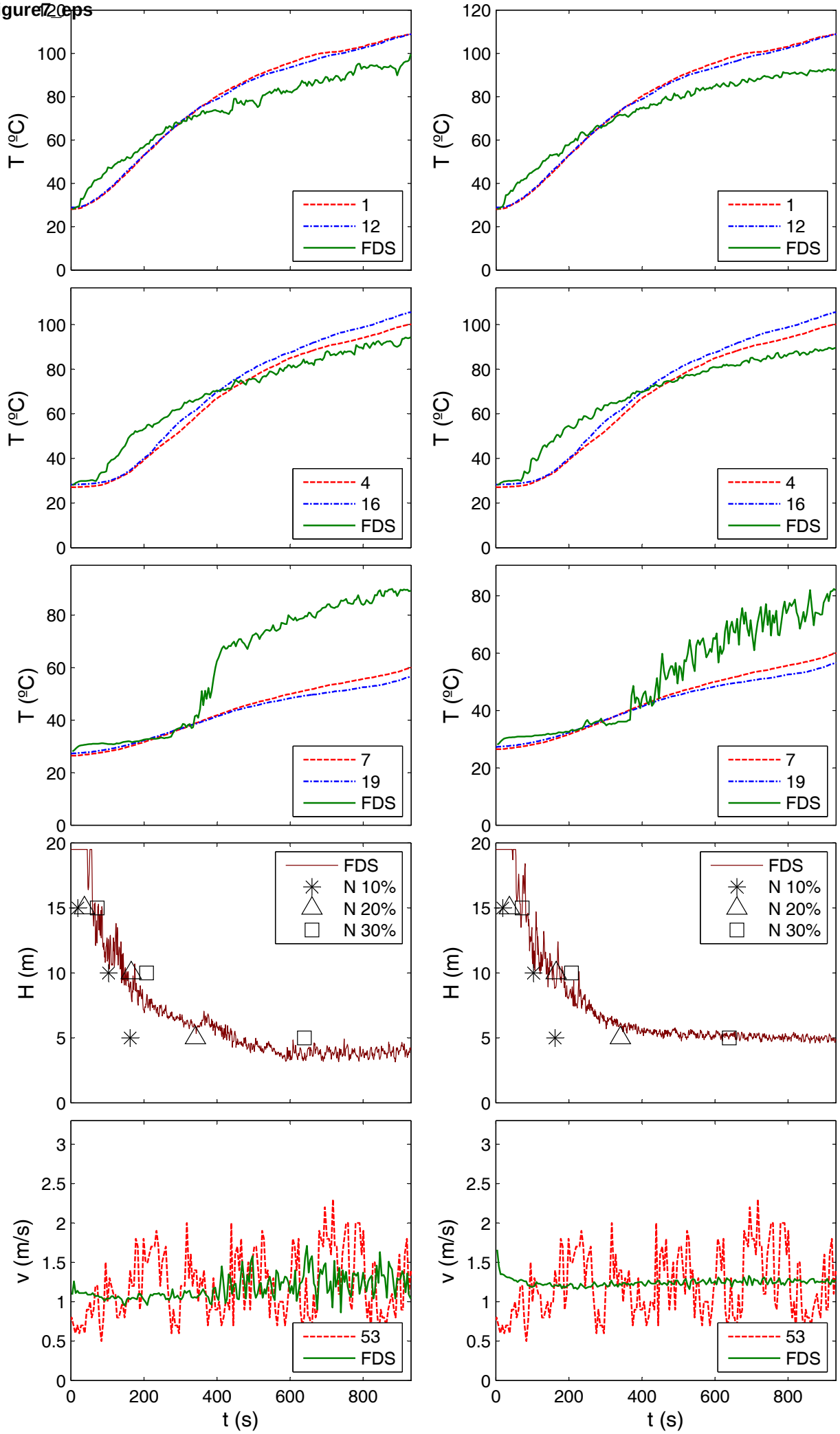

Figure8_eps

Figure9_eps

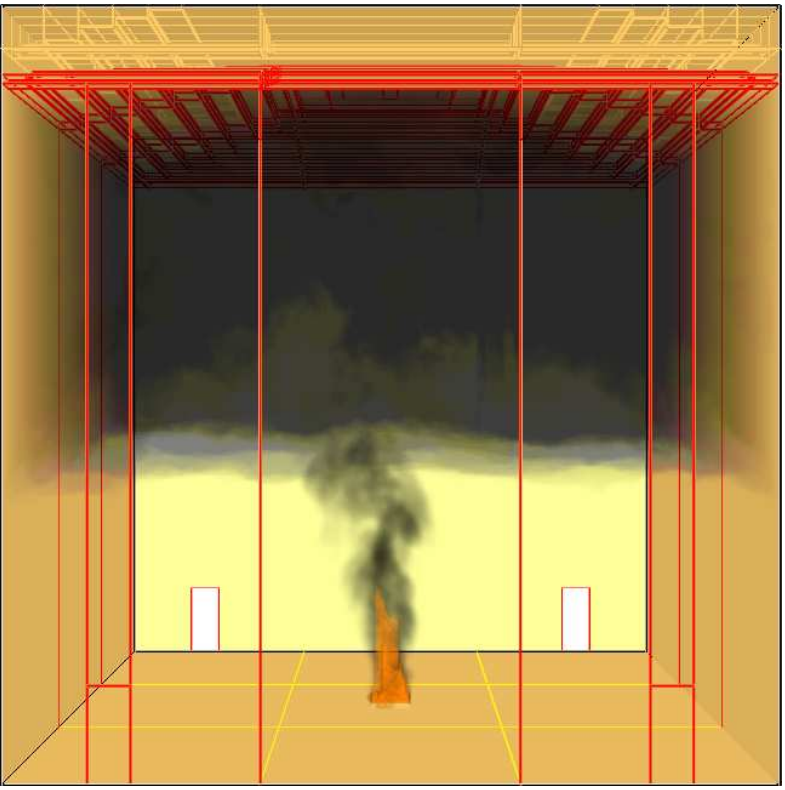

t = 150s

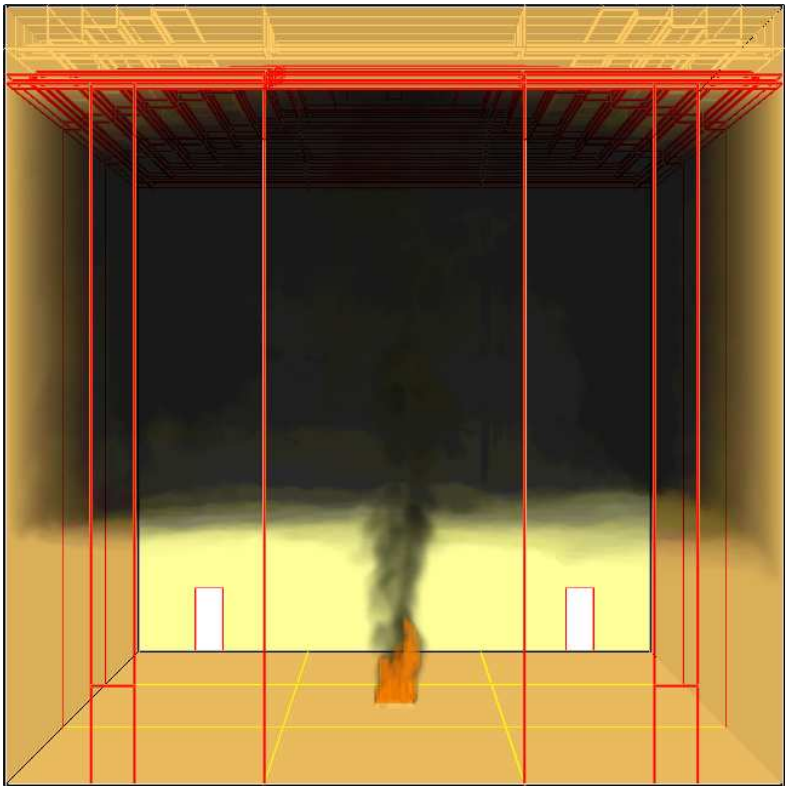

t = 250s

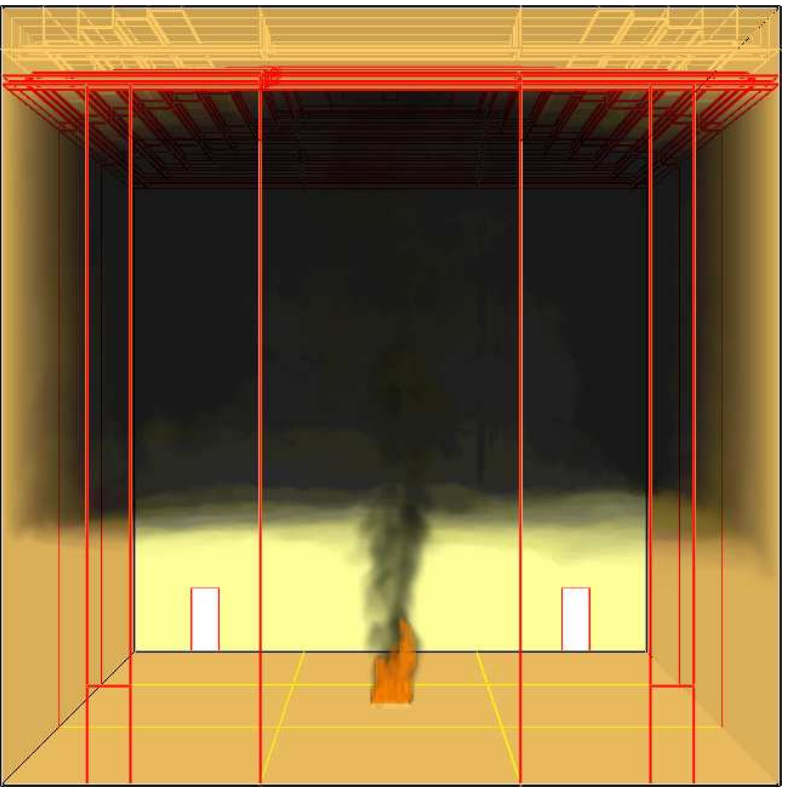

t = 350s

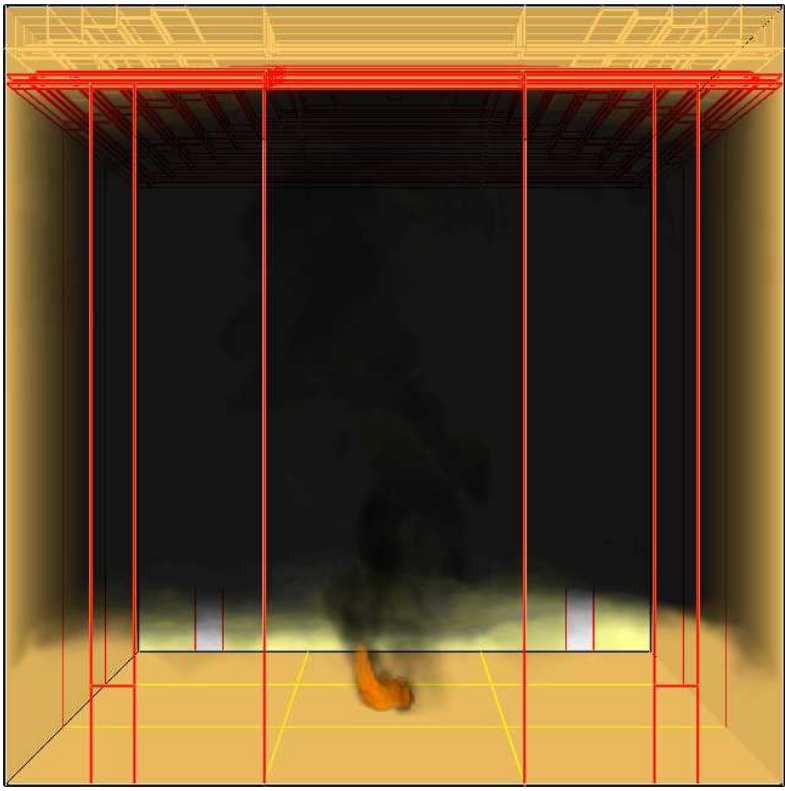

t = 450s

Figure10_eps

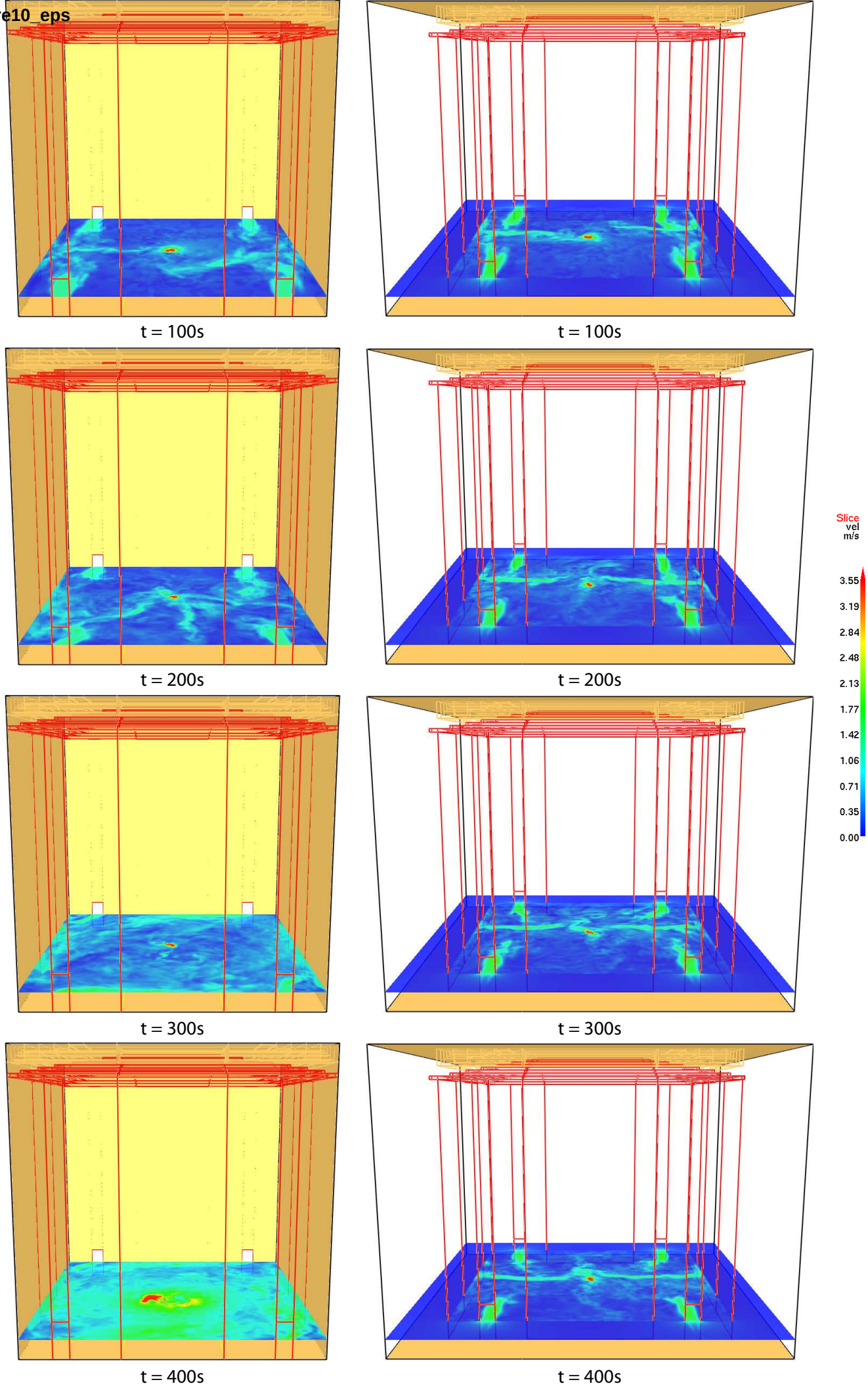

Figure11_eps

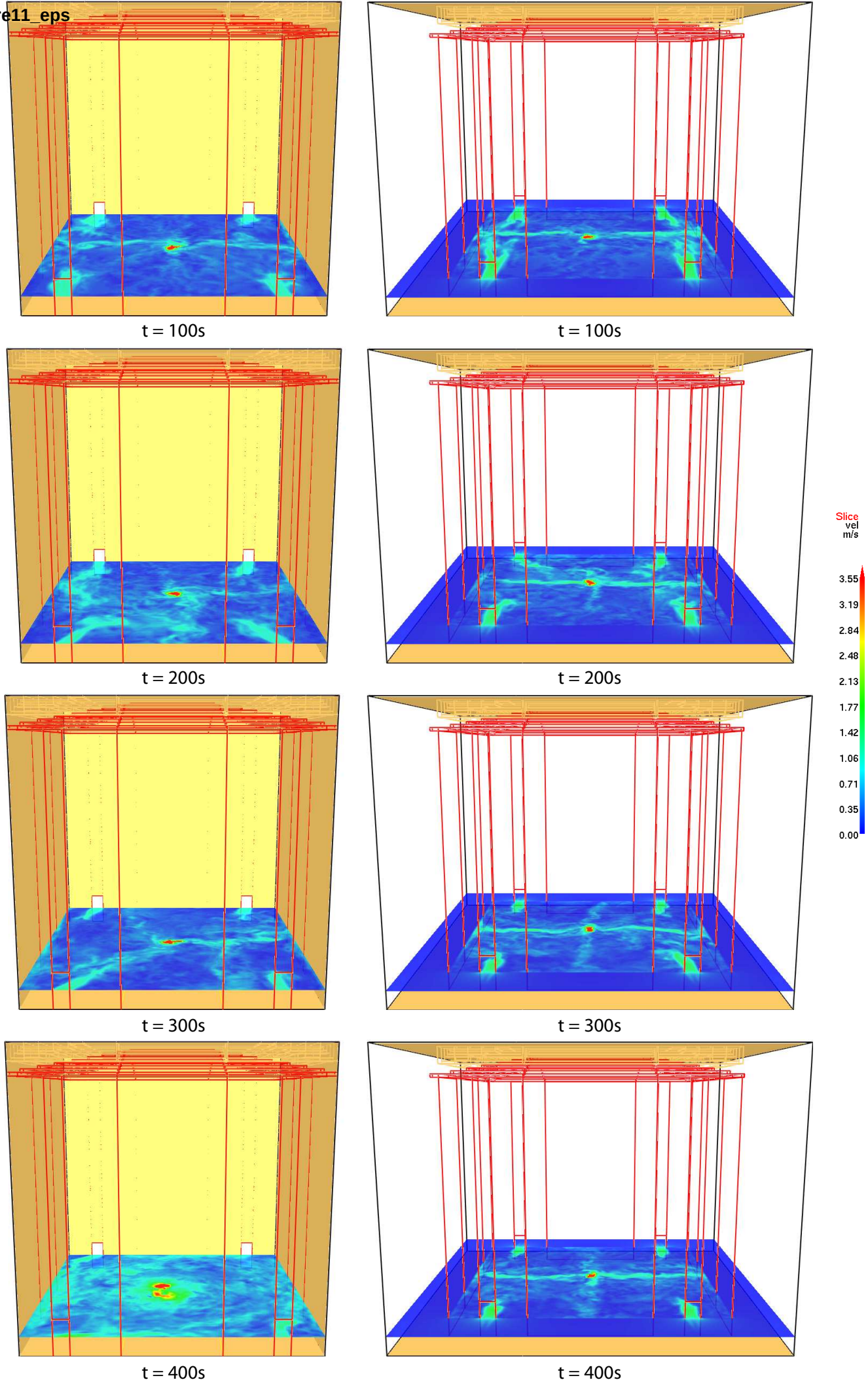

Figure12_eps

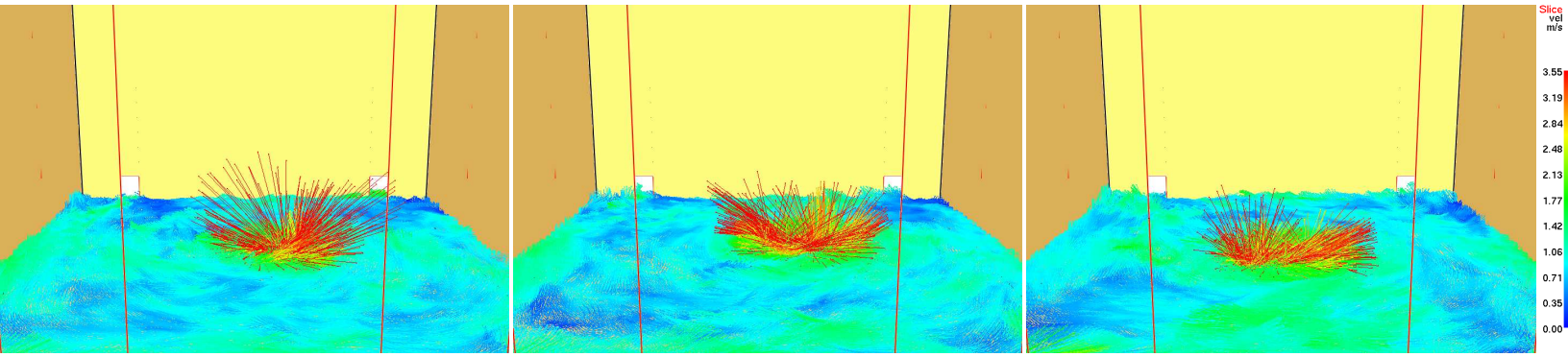

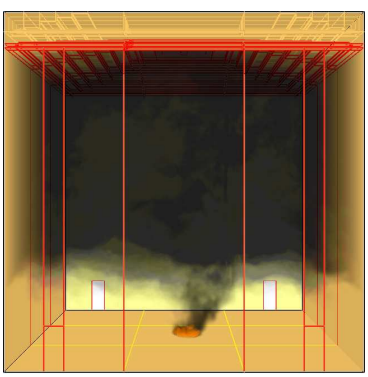

t = 445.3 s

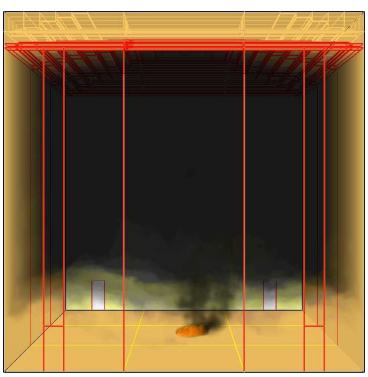

t = 730.8 s

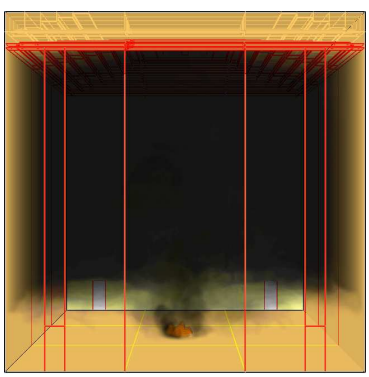

t = 1062.3 s

Figure13_eps

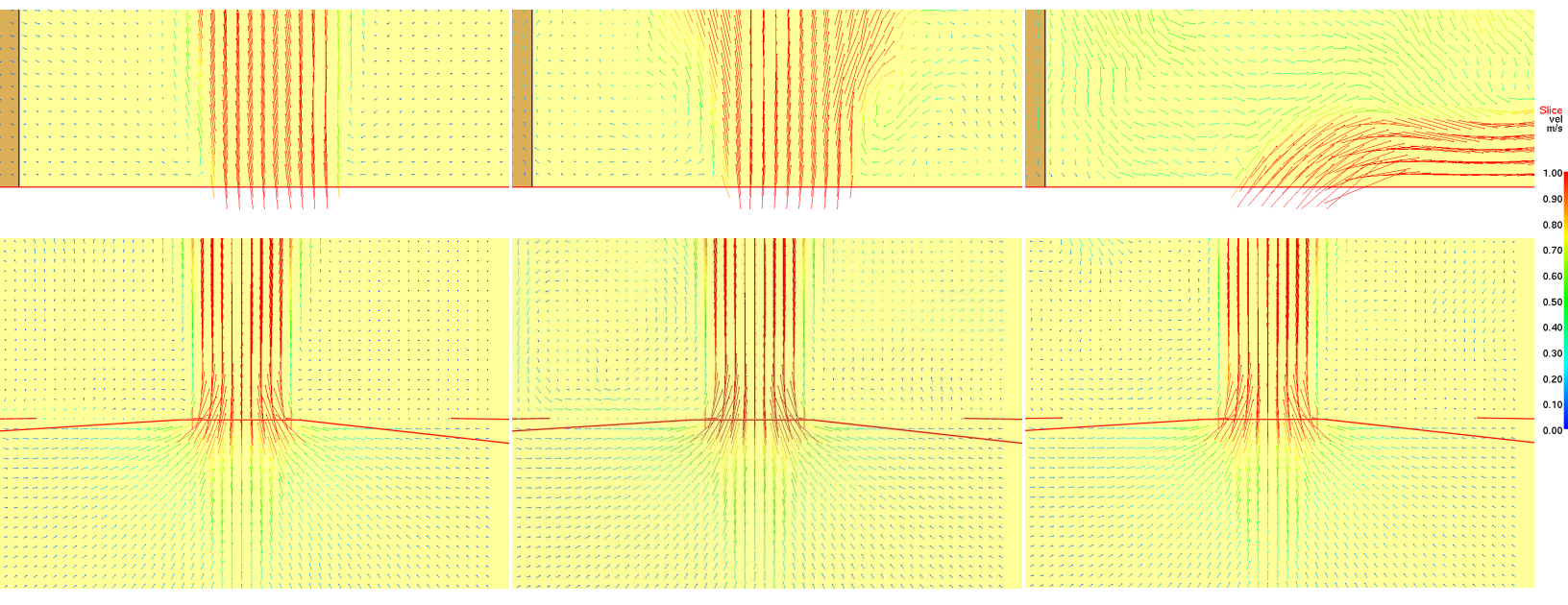

t = 50.3 s t = 151.0 s t = 250.5 s

Figure14_eps

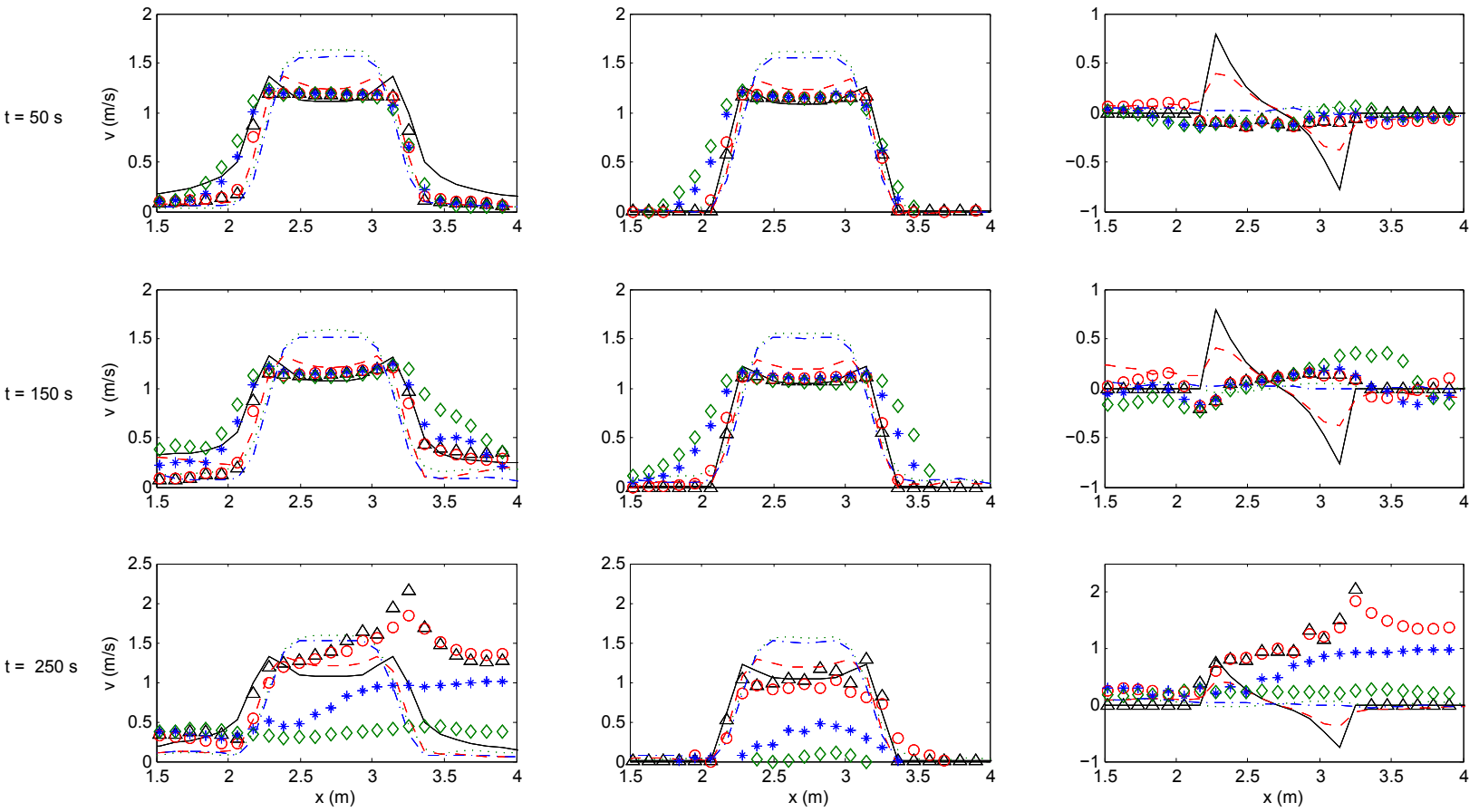

Figure15_eps